Recent Advances in Solid-State NMR Spectroscopy

Sharon E. Ashbrook[1]*, John M. Griffin[2] and Karen E. Johnston[3]

[1] *School of Chemistry, EaStCHEM and Centre of Magnetic Resonance, University of St Andrews, St Andrews, KY16 9ST UK*

[2]*Department of Chemistry and Materials Science Institute, Lancaster University, Lancaster, LA1 4YB UK*

[3] *Department of Chemistry, Durham University, South Road, Durham, DH1 3LE UK*

*Author to whom correspondence should be addressed.

E-mail: sema@st-andrews.ac.uk

Invited article for *Ann. Rev Anal. Chem.*

Abstract

The sensitivity of NMR spectroscopy to the local atomic-scale environment offers great potential for the characterisation of a diverse range of solid materials. Despite offering more information than its solution-state counterpart, solid-state NMR has not yet achieved a similar level of recognition, owing to the anisotropic interactions that broaden the spectral lines and hinder the extraction of structural information. Here, we describe the methods available to improve the resolution of solid-state NMR spectra, and the continuing research in this area. We also highlight areas of exciting new and future development, including recent interest in combining experiment with theoretical calculations, the rise of a range of polarisation transfer techniques that provide significant sensitivity enhancements and the progress of *in situ* measurements. We demonstrate the detailed information available when studying dynamic and disordered solids, and discuss the future applications of solid-state NMR spectroscopy across the chemical sciences.

Keywords: Solid-state NMR, NMR crystallography, *in situ*, high-resolution spectroscopy, sensitivity enhancement

1. Introduction

Since its introduction over 70 years ago,(1,2) nuclear magnetic resonance (NMR) spectroscopy has established itself as one of the most widely used analytical tools in the chemical sciences, providing an element-specific and non-destructive measurement that is applicable to many phases. However, solid-state NMR spectroscopy(3-5) has struggled to match the resolution of its solution-state counterpart, owing to the orientational dependence (anisotropy) of the interactions that affect the nuclear spins. These include the chemical shielding (arising from the interaction with the surrounding electrons), and interactions between nuclear spins, both through bonds (J coupling) and through space (dipolar coupling).(3-5) These interactions lead to significant broadening of the spectral lineshapes, as shown in Figure 1, which is absent in solution owing to the rapid molecular tumbling. This has resulted in a considerable and ongoing effort to improve the sensitivity and resolution of solid-state NMR spectra, by averaging or removing the anisotropic components of the interactions present. Such efforts have resulted in increasing applications of solid-state NMR spectroscopy to problems across the chemical, physical and biological sciences.

Determining structure in the solid state is a crucial pre-requisite to understanding the structure-property relationship and, therefore, to the design of new materials with improved performance. In many cases, the solid state is typified by a periodically repeating structure, and is often studied using diffraction-based methods that rely on long-range order. However, many useful properties arise from some variation in the periodicity, including changes in the nature of an atom/molecule occupying a particular position, variation in the position of functional groups or molecules in different parts of a material, or some dynamic (time-dependent) structural change. In this context, a spectroscopic approach enables the local structural environment to be studied in detail, without any requirement for long-range order. Information on coordination numbers, coordinating atoms, covalent bonding, through-space interactions between atoms/molecules and dynamics on timescales that span 15 orders of magnitude are readily available using NMR spectroscopy, in contrast to the (length and time) averaged

structural picture produced by diffraction.(3-5) Diffraction and NMR spectroscopy, therefore, provide complementary approaches for structural characterisation, and enable a more detailed picture to emerge. This has been exploited in recent years in the emerging field of NMR crystallography,(6-7) where spectroscopic information is used alongside diffraction to solve, or more usually refine, solid-state structures. This is often facilitated by the use of first-principles calculations, enabling prediction of the NMR parameters from a structural model, and providing a link between diffraction-based models and the predicted NMR observables.(8-9) Recent developments in the use of periodic boundary conditions in these calculations(10-11) have opened up the study of solids, and significantly increased the potential impact of this area.

Here, we will review some of the most recent advances in the field, including development of more advanced NMR methodology, the ongoing aim to increase sensitivity, improvements in theoretical calculations, and highlight some of the more challenging areas of application – including disordered and dynamic materials and *in situ* studies. Finally, we conclude by considering where the future advances will take this field and the challenges that remain. Clearly, we cannot hope to provide a comprehensive review of such a large area, and we will highlight more specialist reviews in each section.

2. Advanced Methodology and Challenging Systems

In order to extract detailed structural information from NMR spectra of solids, high resolution is required. This is most commonly achieved using magic-angle spinning (MAS),(3-5,12) involving rapid rotation of the sample around a fixed ("magic") angle of 54.736°. MAS is able to remove the interactions that affect I = 1/2 nuclei, providing sample rotation is sufficiently rapid, and so can, in principle, produce the desired high resolution. This can be seen in Figures 1a-c, where the resolution of the ^{1}H spectrum of theobromine is significantly improved as the MAS rate increases.

For nuclei with higher spin quantum number (I > 1/2) MAS is not able to remove completely the interaction between the nuclear quadrupole moment and the surrounding electric field gradient, and spectra remain broadened even under rapid sample

rotation.(3,14,15) In principle, the lineshapes can provide information on the magnitude (C_Q) and the asymmetry (η_Q) of the quadrupolar interaction, and therefore on the surrounding field gradient. However, in practice, it can be difficult to deconvolute the overlapped spectral lineshapes. Over 75% of NMR-active nuclides are quadrupolar, and there has been considerable effort to address this issue over the last 30 years, with approaches developed to remove completely the quadrupolar broadening.(3,13-21) Early methods exploited sample rotation around two different angles, simultaneously for double rotation (DOR),(13,15) where one rotor spins inside a second, and sequentially for dynamic angle spinning (DAS).(13,16) Although successful, these approaches require specialist and expensive hardware and, for DOR, sample spinning rates are limited by the complex rotor design. NMR of quadrupolar nuclei was revolutionised in 1995 by the multiple-quantum (MQ) MAS experiment,(13,17,18) which was able to provide high-resolution spectra for quadrupolar solids, using only conventional hardware. This two-dimensional experiment involves the correlation of different transitions in the spin system (*i.e.*, triple- and single-quantum), resulting in a spectrum that is able to separate the different contributions from different species, as shown in Figure 2a for an aluminophosphate framework.(19) Although MQMAS is easy to implement, it suffers from inherently poor sensitivity. Alternatively, the satellite-transition (ST) MAS experiment is similar in design but utilises only single-quantum satellite transitions (*i.e.*, $m_I = \pm 3/2 \leftrightarrow m_I = \pm 1/2$, etc.,) and has much better sensitivity.(13,20,21) However, the difficulty of its experimental implementation, requiring the spinning angle to be set to a very high accuracy (±0.004°), has limited its wide application.

Despite the availability of faster MAS rates (*e.g.*, 111 kHz now available commercially), the concomitant decrease in sample volume (*e.g.*, 0.7 mm rotor diameter) reduces sensitivity, and often restricts applications to nuclei with high sensitivity. In many other cases, spectral resolution is improved through a combination of MAS with decoupling, where radiofrequency (rf) pulses are applied to remove the dipolar couplings between spins.(3,22,23) This is relatively straightforward for heteronuclear couplings, as pulses can be applied to one spin while observing the signal from another. The simplest approach involves continuous irradiation (continuous-wave decoupling), although more

sophisticated sequences, which perform more efficiently at differing MAS rates, or when larger anisotropic interactions are also present, have been heavily investigated.(22) Homonuclear decoupling is particularly challenging, involving simultaneous irradiation and observation of the same spin. This problem has been addressed by "windowed" sequences, where series of pulses periodically average the homonuclear dipolar coupling to zero, enabling a data point to be acquired, and the acquisition of signal one data point at a time.(23) An example is shown in Figure 1d, where homonuclear decoupling (using DUMBO (24)) even at relatively slow MAS rates significantly improves the spectral resolution. As hardware improves (*e.g.*, faster MAS rates and higher rf field strengths) and higher magnetic fields become available, optimised decoupling sequences are being introduced, leading to significant improvements in resolution and the information that can be obtained.

Although interactions between spins can result in broadened spectral lines, the ability to "connect" two spins in this way provides vital structural information. These interactions are exploited in magnetisation transfer experiments, which provide information on through-bond connectivity and through-space proximity of spins. Simple approaches include cross polarisation (CP),(3,25) where transfer of magnetisation from an abundant high-γ nucleus can be used to enhance the sensitivity of a less abundant, lower-γ nucleus, and to edit the spectrum on the basis of the spatial proximity of the two spins. Many methods use two-dimensional spectroscopy, where the presence of a cross peak indicates magnetisation transfer (and, therefore, an interaction) between two spins, and spectral intensities can provide information on the number of covalent bonds or distance between the two species. A number of experiments have been available for spin I = 1/2 nuclei for many years(26) and, more recently, these have been extended to quadrupolar nuclei(27), with many adapted to achieve high resolution in combination with MQMAS. Most recently, two-dimensional experiments that exploit magnetisation transfer to enable indirect detection of signal for more challenging nuclei, such as ^{14}N, ^{15}N and ^{35}Cl,(28,29) have been introduced. An example is shown in Figure 2b,(30) where indirect detection is used to obtain the ^{15}N NMR spectrum of a pharmaceutical compound. Particularly for quadrupolar nuclei, the ability to synchronise acquisition with sample spinning in the

indirect dimension of an experiment (as opposed to in real time) enables a much simpler spectrum, without a manifold of spinning sidebands present, to be acquired. Although J couplings have an isotropic component (and therefore survive MAS), the averaging of the dipolar interaction under sample spinning can impact on the efficiency of any through-space transfer of magnetisation. Elegant work by Levitt and co-workers over the last few years has demonstrated that interactions can be "recoupled" through the application of multi-pulse sequences (exploiting their different real- and spin-space symmetries), significantly improving sensitivity.(31)

If the anisotropic broadening is significant (*e.g.*, for nuclei subject to a very large quadrupolar interaction), it may not be possible to employ MAS at a sufficiently rapid rate. In these cases, it is preferable to acquire "wideline" spectra on a non-rotating sample.(32) While accurate NMR parameters can be determined, and information on interactions typically averaged by MAS is also available, the lower resolution can limit the detailed information available as the number of distinct species present increases. To ensure uniform excitation, extremely broad lines are acquired in a frequency-stepped approach, where a series of sub spectra are acquired with a "stepping" of the transmitter frequency, leading to practically challenging and time-consuming experiments. Recent work, led by Schurko and co-workers,(32,33) has aided wideline experiments, through the implementation of shaped WURST pulses that offer broadband excitation, reducing the time taken for spectral acquisition, or enabling spectra with better sensitivity to be obtained in the same timeframe. An example is shown in Figure 2c,(34), a ^{35}Cl spectrum of a palladium-based catalyst, acquired using a frequency-stepped WURST approach. More recently, an approach that provides broadband CP for wideline spectra (BRAIN-CP)(35) has also been introduced, enabling an increase in sensitivity and the extraction of information on spatial proximities. Further improvements in sensitivity are typically required for the acquisition of wideline spectra, and techniques such as CPMG (Carr Purcell Meiboom Gill) echo trains in acquisition (as used in Figure 2c), or the prior manipulation the population of the nuclear spin energy levels, are routinely employed.(36) Sensitivity enhancement techniques are discussed in Section 3 below.

3. Signal Enhancement

One of the key limitations of NMR spectroscopy is its inherently low sensitivity arising from the small difference in nuclear spin populations at ambient temperatures. Signal enhancement has, therefore, been a constant theme in solid-state NMR method development. As described in Section 2, one of the earliest and most widely used methods for signal enhancement in solid-state NMR is CP, whereby magnetisation is transferred usually from an abundant high-γ spin, such as ^{1}H, or ^{19}F, to a lower-γ, more dilute spin such as ^{13}C or ^{15}N.(25,37) CP transfer takes place *via* the dipolar coupling, and can give a maximum theoretical enhancement of γ_I/γ_S, resulting in a factor of 4 enhancement for CP from ^{1}H to ^{13}C (saving a factor of $4^2 = 16$ in time). In practice, further sensitivity gains are often observed owing to the typically faster T_1 relaxation for abundant high-γ spins, as more transients can be acquired in a given amount of time. Owing to the sensitivity advantages and relative ease of implementation on standard hardware, ^{1}H-^{13}C CP MAS NMR is generally the go-to technique for studying organic and biological materials. However, an important consideration is that the distance dependence of the transfer efficiency means that CP MAS NMR spectra are not strictly quantitative. In cases where quantification is important, the CP dynamics must be accurately taken into account, or more time-consuming direct polarisation experiments are required. Furthermore, for quadrupolar nuclei, the CP spin dynamics are considerably more complex, and efficiency also depends on the quadrupolar parameters, the rf field strength and the MAS rate.(38-40) In many cases, a sensitivity enhancement is not observed, but the approach remains useful for spectral editing or magnetisation transfer within two-dimensional experiments.

Another widely-used signal enhancement technique is CPMG, which consists of a train of echoes following an initial excitation pulse, as shown in Figure 3a.(41,42) For materials with long transverse relaxation times (T_2), many echoes can be acquired, thereby significantly increasing the signal obtained per transient. Fourier transformation of the resulting echo train yields a spectrum containing a series of narrow "spikelets", the intensities of which trace out the NMR lineshape with a much higher signal-to-noise ratio. CPMG has been used widely to enhance signals from spin I = 1/2 nuclei,(43,44) where

broadening can result from large chemical shift anisotropy interactions or chemical shift distributions due to structural disorder. An example is shown in Figure 3b, where ^{89}Y CPMG MAS NMR experiments on $Y_2Zr_{2-x}Sn_xO_7$ pyrochlores provides increased signal-to-noise over more conventional spin echo experiments.(45) A particularly successful application of CPMG has been for the observation of low-sensitivity quadrupolar nuclei. Many nuclei suffer from the multiple challenges of low natural abundance, low gyromagnetic ratio and large quadrupole moments, making them very challenging to observe by conventional NMR approaches. Quadrupolar CPMG(46,47) (or QCPMG) NMR techniques have been highly successful in the study of such nuclei, especially when combined with the advantages of high magnetic fields. Figure 3c illustrates this for orthoenstatite ($MgSiO_3$), which contains two crystallographically-distinct Mg sites, only one of which is observed in the ^{25}Mg MAS NMR spectrum.(48) It is only by recording frequency-stepped CPMG spectra over a much wider frequency range that the severely quadrupole-broadened second site can be observed.

Another area where sensitivity is a particular problem in solid-state NMR is the popular MQMAS experiment,(17,18) owing to the inherently inefficient excitation and conversion of triple-quantum coherences. As described in Section 2, this problem can be addressed by using the more sensitive STMAS(20,21) experiment; however, STMAS is also significantly more challenging to implement. In view of this, significant effort has been devoted to optimisation of MQMAS. One successful approach is to combine MQMAS with CPMG to enhance the directly-acquired signal.(49) A large amount of work has also been performed to increase the inherently poor efficiency pulse that converts triple- to single-quantum coherences by replacing it with more sophisticated pulses or groups of pulses. One of the most commonly employed approaches is the use of a double frequency sweep (DFS).(50) This consists of a single pulse swept across a wide frequency range to saturate/invert the satellite transitions. This has the effect of efficiently transferring triple-quantum coherences to single-quantum coherences and can provide typical signal enhancement factors of 2-3, corresponding to experimental time savings of 4-9. Another widely used approach is fast amplitude modulation (FAM) which is used in a similar way to DFS but, rather than a single pulse, comprises a series of phase-alternating rectangular

pulses.(51,52) In principle, the signal enhancement of DFS and FAM-based pulses depends on several factors including the C_Q, the crystallite orientation and MAS rate, and can require time-consuming experimental optimisation to maximise signal enhancement. Recently, Ashbrook and co-workers have introduced the FAM-N approach, where the number and durations of the components of a FAM pulse can be computationally optimised prior to experiment.(53,54) This approach gives pulses that can be used without further optimisation and are robust to variations in nutation rate and C_Q, making them applicable to a wide range of materials.

In recent years, considerable attention has been focused on the development of alternative methods for solid-state NMR signal enhancement based on hyperpolarisation of nuclear spin-states. One of the most promising methods is dynamic nuclear polarisation (DNP),(55,56) whereby the large polarisation of unpaired electrons is transferred from external mono- or biradical species to NMR-active nuclei in the sample. The DNP enhancement depends upon γ_e/γ_n, where γ_e and γ_n are the respective gyromagnetic ratios of the electron and polarised nucleus, meaning enhancement factors of up to 658 can theoretically be obtained for ^{1}H. In practice, enhancement factors > 20 can be routinely observed, which can dramatically reduce experimental times and permit experiments which are unfeasible without DNP enhancement. An example is shown in Figure 3d for cyclic diphenylalanine nanotubes. Here, DNP provides a ^{13}C signal enhancement of 25, as determined by the intensity ratio of spectra recorded with and without microwave irradiation.(57) This corresponds to a saving of 625 in experimental time, enabling ^{13}C-^{13}C through-space correlation experiments to be recorded at natural abundance in a few hours.

In a typical DNP-enhanced solid-state NMR experiment, the powdered sample is prepared by impregnation with a solution containing a radical species such as TOTAPOL or bTbK.(58,59) Experiments are performed with MAS at low temperatures (typically ~100 K) to freeze the solvent and increase the polarisation of the unpaired electrons. Polarisation transfer is achieved by irradiation with a high-power microwave source. The microwave frequency is chosen to take into account the properties of the radical used and the different polarisation transfer mechanisms that are possible.(55,56). In principle, DNP

enhancements are possible for any nucleus; however, in practice the electron polarisation is generally transferred directly to ^{1}H in the solvent, and CP is subsequently used to transfer this polarisation to heteronuclei in the sample.

DNP-enhanced solid-state NMR is still at an early stage, but has already been demonstrated for a wide range of materials including oxides, pharmaceuticals and polymers.(55,56) DNP shows promise to enable experiments that are unfeasible under conventional conditions. This includes the possibility to perform NMR experiments on species with low natural abundance, such as ^{17}O (60,61) and ^{2}H,(62) without the need for expensive isotopic enrichment. Additionally, since the polarisation transfer occurs from species external to the sample, the DNP enhancement is highly surface selective. Surfaces and interfaces are very difficult to study by conventional solid-state NMR because they usually make up only a very small proportion of the total sample. The ability of DNP to selectively enhance surface signals opens up new possibilities for studying materials, particularly porous solids and catalysts where the external surface structures are central to the properties observed.

4. Investigating Disorder and Dynamics

The high sensitivity of NMR to the local chemical environment makes it a powerful probe of disordered materials, where the structure and/or composition may vary locally throughout the sample. The effect on the NMR spectrum depends on the nature of the disorder and the properties of the nucleus being studied.(63) For the case of positional disorder (*e.g.*, as is present in a glass or polymer), the overall structure will typically contain a continuous distribution of local bonding and coordination environments. This results in continuous distributions of chemical shifts, leading to broadening of the resonances and loss of spectral resolution. However, providing the broadening is less than the chemical shift difference between different distinct types of chemical environments, it is usually possible to deconvolute the lineshapes to gain quantitative information about the populations of different bonding environments.

In the case of compositional disorder, where local variations in composition or site occupancy are present within an otherwise crystalline structure, solid-state NMR spectra of the substituted species can provide detailed information into the local environment and substitution mechanism. Substituted species residing in different environments within the material will generally exhibit different chemical shifts (or quadrupolar parameters), which can be linked to the local structure through theoretical calculations (see Section 5). Often, substitution can lower the symmetry, resulting in a more complex but information-rich NMR spectrum than may be expected on the basis of the underlying (or average) crystal structure. An example of this is shown in Figure 4a, a ^{19}F MAS NMR spectrum of a disordered fluorinated-substituted hydroxyl silicate.(64) In this material, fluorine substitutes for hydroxyl groups on one crystallographic site, but owing to the "chain-like" arrangement of the these in the structure, four different ^{19}F local environments are observed. The different intensities of the four lines shows that the substitution is not completely random, and fluoride ions have a preference to substitute adjacent to hydroxyl groups, forming F…H–O hydrogen bonds. In addition to studying the substituted species, other "spectator" species present in compositionally-disordered systems can also yield information. This is illustrated in Figure 4b, which shows a ^{89}Y MAS NMR spectrum of the pyrochlore ceramic, $Y_2Ti_{1.2}Sn_{0.8}O_7$.(65,66) In this material, Y is surrounded by six next nearest neighbour (NNN) sites, which can be occupied by either Sn or Ti, leading to the observation of multiple spectral resonances. Through deconvolution and integration of the resonance intensities, it is possible to extract information on the Sn/Ti cation distributions.

For nuclei with spin quantum number $I > 1/2$, changes in the local structural environment result in a variation of both the chemical shift and the quadrupolar interaction.(63) This leads to additional broadening of the spectral lineshapes, and changes in their shape, with a characteristic "tail" to lower frequencies typically observed. It can be difficult to obtain information on the nature and magnitude of the distributions of different NMR parameters present from a simple MAS spectrum, but the shape of the spectral resonances in MQMAS (or STMAS) spectra can provide more detailed insight. It is possible, using freely-available analysis packages,(67) to fit the two-dimensional lineshapes (typically assuming a Czjzek(68,69) distribution of the field gradient and a

Gaussian distribution of the chemical shift) and extract information on the magnitude of the distribution of the NMR parameters.

In addition to "static" disorder, NMR can be used to probe "dynamic" disorder, where the locations of atoms, chemical groups or molecules change with time. The range of NMR interactions means enable the study of dynamics over a very wide range of timescales, in principle from ~10^{-12} s^{-1} to ~10^{3} s^{-1}. Faster processes can be probed using spin-lattice, or T_1, relaxation time measurements.(3,70) The mechanism of T_1 relaxation relies on fluctuations in the local magnetic field at frequencies comparable to the Larmor frequency, which is typically on the order of several tens or hundreds of MHz. Therefore, variable-temperature T_1 measurements can detect the presence of molecular or ionic motions in this range (*i.e.*, on nano- to picoseconds timescales). Much slower motion (on the timescale of milliseconds to seconds) can be studied by two-dimensional exchange experiments involving a "mixing time", chosen to be comparable to the timescale of the motion.(3,70) Molecular motion or exchange of species between different environments during this time will result in a NMR frequency difference that is detected as a correlation in the spectrum. Through analysis of the intensities of such correlation peaks as a function of mixing time, the exact timescale of the motion can be determined.

Intermediate timescale motion can be probed through a range of NMR experiments on different nuclei, depending on the species present in the material. One nucleus that has been very widely used for the study of dynamics in organic materials is ^{2}H, which typically exhibits quadrupolar interactions in the range 100 – 200 kHz, meaning that it is sensitive to dynamics on the microsecond timescale.(71) The effects of dynamics are observed as changes in the appearance of the lineshape measured for a static sample at different temperatures. This is illustrated in Figure 4c for the case of a deuterated metal organic framework.(72) As the rate of motion increases with increasing temperature, the quadrupolar interaction becomes partially averaged, resulting in changes in the width and positions of singularities in the lineshape. Comparison with simulated ^{2}H NMR lineshapes for different types of molecular motion reveal that the observed changes are consistent with "π-flipping" of the rings in the terephthalate linkers.

While static ^{2}H NMR experiments have been most widely used for the study of dynamics, ^{2}H MAS NMR can also provide important dynamic information. In principle, MAS should perfectly average the ^{2}H first-order quadrupolar interaction, resulting in a spectrum consisting of narrow isotropic resonances and spinning sidebands. However, if the molecular motion occurs on the same timescale as the rotation of the sample (typically 10 – 100 μs), it can interfere with the averaging of MAS and lead to broadening of resonances. MAS can therefore be used to study materials with subtle molecular motions where small broadenings of the relatively narrow MAS linewidth are easier to detect and measure than equally small changes in the static powder pattern lineshapes.(70,73)

In general, the motion of any species within a material will not only modulate its own magnetic environment, but also that of nearby atoms and molecules. Therefore, in a similar way to the study of static disorder, it is not always necessary to directly study the atom or molecule undergoing the dynamic process, and it is, in some cases, the "spectator" species that provide more detailed dynamic information. This is particularly true in framework materials, where guest species may be highly dynamic inside the pores, resulting in detectable effects on nearby framework species. As shown in Figure 4d, the dynamics of guest species within the aluminophosphate AlPO-34 can have a profound effect on ^{27}Al MAS NMR spectra of the porous framework.(74) In this experiment, modulation of the ^{27}Al local environment by motion of the nearby guest species leads to either broadening or narrowing of the ^{27}Al satellite transition sidebands, depending on the timescale of the motion. Comparison of variable temperature ^{27}Al MAS NMR spectra of different forms of AlPO-34 revealed different motional regimes, linked to the presence of H_2O that accompanies some guest species inside the framework pores.

5. Calculations and NMR Crystallography

The term "NMR crystallography" initially described the use of NMR spectroscopy to determine structural information.(6) However, in recent years it has been extended to cover a wide array of approaches to structural determination, refinement, selection or validation, in which NMR data is used in conjunction with diffraction, first-principles

calculations and other spectroscopic techniques.(7-9,75-77) In recent years, the field of NMR crystallography has been driven both by the advancement of NMR spectroscopy, and the development of computational codes based on density functional theory (DFT) that enable NMR parameters to be accurately calculated for real systems.(8,9)

Until relatively recently, the prediction of NMR parameters using quantum-chemical calculations was predominantly applied to molecular systems. Using this approach, periodic solids are modelled as a cluster of atoms centred on the atom of interest, with any "hanging" bonds terminated typically with H. Although this approach can work well for some systems (most notably, molecular solids), it has several limitations, including the accuracy of the final structural model and the high computational costs associated with large-scale cluster calculations. The use of a periodic approach, in which the three-dimensional structure is recreated from a single unit cell by exploiting the inherent translational symmetry of the solid state, enables all atoms in a system to be calculated accurately and simultaneously. The introduction of the gauge-including projector augmented wave (GIPAW) approach(10) has revolutionised the use of calculations among the experimental solid-state NMR community.(8,9) This planewave pseudopotential approach enables the straightforward and accurate calculation of NMR parameters, including the chemical shielding, quadrupolar interactions and scalar couplings.(10,11) To date, the combination of experimental NMR experiments and DFT calculations has been successfully demonstrated for a wide array of systems, including minerals, ceramics, porous framework materials, pharmaceuticals, co-crystals, layered systems and energy materials.(8,9,19, 75-82)

To successfully calculate or predict NMR parameters, an accurate structural model is an essential pre-requisite. Models can be generated from experiment (typically using diffraction methods) or computationally (by modification of a known structure or *via* crystal structure prediction (CSP) methods). The accuracy of the initial model will vary depending on how it is generated, *e.g.*, from single crystal or powder X-ray or neutron diffraction data. In many cases, the models produced require optimisation of the unit cell parameters and/or atomic positions, as they differ from the lowest-energy DFT structure(s). The importance of geometry optimisation prior to calculation of the NMR

parameters has been discussed extensively in the literature.(8,9,19,83,84) Occasionally, when models are obtained from neutron diffraction, geometry optimisation may not be necessary, as has been demonstrated for porous materials(85) and glucose.(86)

Many molecular systems are bound by dispersion interactions and the underestimation by some DFT methods can have a significant effect on the optimisation of structural models. This is particularly important for systems such as molecular solids or metal-organic frameworks (MOFs) and aluminophosphates (AlPOs), where the structure can "fall apart", or the geometry can be substantially altered, during optimisation. This can result in an overestimation of interatomic distances or unit cell dimensions, and, hence, inaccurate results.(8,9,87) In recent years, several approaches have been developed to include dispersion interactions within DFT calculations, including hybrid density functionals(88) and semi-empirical dispersion correction (SEDC) schemes.(89,90) The successful application of such methods has been demonstrated in recent years *via* the modelling of adsorption or surface interactions(91,92) and framework materials.(87,93)

In cases where structures cannot be determined from experiment, it is possible to generate candidate crystal structures using computational methods and compute the associated NMR parameters for structural verification. Two such methods were recently proposed, the first of these s the CSP method of Day,(94) in which an isolated molecule is first subjected to a conformational search under molecular mechanics (MM). Loosely packed crystal structures of rigid molecules are then generated through Monte Carlo simulations, the most stable of which are isolated and optimised through a hybrid DFT/MM approach and ranked according to their energy. The second approach, the AIRSS method of Needs and Pickard,(95) produces structures from randomised unit cell vectors and atomic coordinates. The structures are optimised under quantum-mechanical stresses and forces. AIRSS can be used in conjunction with GIPAW calculations *via* periodic codes such as CASTEP,(96) as recently demonstrated by Mayo and Morris for battery materials(97) and Moran *et al.* for silicate minerals.(98) The latter study, as shown in Figure 5, investigated the hydration of wadsleyite (β-Mg_2SiO_4),(98) a mineral present in the inner Earth. After removing a Mg3 cation (for charge balance) from the anhydrous structure, two protons were placed randomly within the cell and the forces upon them

minimised using DFT. This process was repeated, generating 819 structural models that were ranked by their energy, and NMR parameters are predicted and compared to experiment(99) to determine the structural motifs present in the disordered mineral.

For ordered systems, DFT calculations are typically used to assign and interpret NMR spectra. However, they can also be used to predict NMR spectra (and therefore direct future experiments, as in Figure 3c), and to understand the influence of structural changes on observable NMR parameters. Increasingly, however, calculations are being used in conjunction with experiments to gain insight into disordered systems. There are several ways in which disorder (compositional or positional) can be modelled using calculations. In all cases, a series of possible structural models are generated (depending on the extent and type of disorder) and NMR parameters predicted and compared to experimental measurements.

For low levels of compositional disorder, simple models can be constructed by substituting a single atom into the structure of a pure end member.(8,9,63) Using this method, it is possible to gain insight into both the NMR parameters for the substituted atom and those that surround it. For cases where very low levels of disorder are present, better approximations may be obtained by constructing supercells. Whilst this method ensures that any substituted atoms are sufficiently isolated and minimises the effects of any structural changes on the neighbouring cells, the computational costs can be high owing to the number of atoms that need to be treated explicitly. If there are multiple possible sites for substitution, a series of calculations would then be required (either single cell or supercell), with different arrangements of the atoms. In all cases, full optimisation of the structure is necessary, as the arrangement of atoms within the unit cell no longer corresponds exactly to any experimental measurement.

Similar approaches can be used to model positional disorder, with sets of candidate structures created by varying the atom positions and their relative distribution.(8,9,63) It should be noted that the extent of disorder exhibited can vary considerably depending on the system, from small changes in the bond lengths and angles to the significant disorder encountered in glasses. In recent years, a number of studies have successfully combined solid-state NMR experiments with DFT calculations to model and understand disorder in

a range of systems, including brownmillerite phases, ceramics, perovskites, layered silicates and framework materials.(8,9,80,81,100-103)

To date, the vast majority of studies have been limited to diamagnetic solids. However, more recently, paramagnetic effects have been employed to gain structural insight into inorganic samples. NMR crystallography methods have been applied to inorganic systems with low concentrations of paramagnetic ions, including pyrochlores, garnets and simple oxides.(104) For example, Seymour *et al*. recently characterised local oxygen environments in Li_2MnO_3 *via* ^{17}O NMR and DFT calculations.(105) This work identified additional ^{17}O resonances caused by stacking faults within the structure.

Although the field of NMR crystallography is still relatively early in its development, the growing interest of experimentalists is driving the demand for more accurate theoretical approaches and the relevance to real systems, *e.g.*, the inclusion of temperature effects. Ultimately, the increasing complexity of the systems under study will require advances the field, both experimentally and computationally.

6. *In Situ* NMR

Although solid-state NMR is a powerful and versatile tool that plays a crucial role in our understanding of the structural and dynamic properties of solids, experimental strategies capable of monitoring reactions in their native environment or under normal working conditions are essential as they can provide real time information on reaction mechanisms, the products formed and the presence of any short-lived reaction intermediates or transition states.(106) In general, the development of *in situ* methods in solid-state NMR has lagged behind many other techniques, such as X-ray and neutron diffraction, IR and Raman spectroscopy,(106) due to the technical challenges associated with adapting the hardware required for high-resolution experiments (*i.e.*, rapidly rotating samples contained in a sealed NMR rotor within a confined and relatively inaccessible space inside a probehead). However, in recent years, a number of *in situ* techniques have been developed, with specific hardware (both sample containers and probes) designed for reactions requiring specialist conditions.(107-111)

In situ methods can provide new insights into the fundamental aspects of crystal nucleation and growth processes, including information on how and when solid phases are formed, the discovery and time evolution of new polymorphs and transformations between polymorphs. In particular, the early stages of crystal growth cannot easily be monitored using diffraction-based approaches, with little or no long-range order present, and variation primarily in the local structural environment. This is shown in Figure 6a, where *in situ* ^{1}H-^{13}C CP measurements follow the crystallisation of glycine from different solvents. The polymorphs produced vary both with reaction time and solvent.(112) In recent years, Harris and co-workers have had considerable success in this area, with the development and implementation of *in situ* methods,(112-114) including the recent Combined Liquid- And Solid-State *In situ* Crystallisation NMR technique, or "CLASSIC NMR" method,(115) where the evolution of both the solid and liquid phases in a heterogeneous system can be probed as a function of crystallisation time. As shown in Figure 6b, interleaved solution- and solid-state spectra are acquired enabling time-resolved spectra to be obtained simultaneously. The use of conventional MAS hardware makes this approach particularly appealing, since many previous *in situ* studies were limited by the difficulties associated with sealing fluids securely inside an NMR rotor such that rapid MAS could be carried out without leakage.(112) In CLASSIC, a homogeneous solution is placed inside a MAS rotor at elevated temperature. By rapidly decreasing to a target temperature, the solution is supersaturated and crystallisation is then thermodynamically favoured.(112,115) This can be monitored as a function of time *via* an alternating cycle of two pulse sequences; one for selectively detecting signal from the solid phase (typically ^{1}H-^{13}C CP MAS NMR) and the other for detecting the liquid phase (usually direct-excitation ^{13}C NMR). Hence, at any one time, signal is selectively detected from only one phase and the other is "invisible" to the measurement.(112,115) Acquiring solid-state NMR spectra of sufficient quality in the shortest time possible is key; hence, optimisation of the sensitivity of the measurement is essential. Improving sensitivity also enables the first small solid particles produced during the crystallisation process to be identified. To date, these techniques have been applied to a variety of systems, including solid inclusion compounds, co-crystals and polymorphic materials.(112-116)

In situ MAS NMR has contributed significantly to the field of heterogeneous catalysis and the fundamental understanding of working catalysts, including their active surface sites and the processes taking place.(117-121) Here, the MAS NMR rotor is used as a microreactor, simulating either batch-like or continuous-flow conditions. The former is typically favoured since it is lower in cost, possible using commercial instruments and enables the whole reaction process to be monitored, including the adsorption of reactants, formation of intermediates and conversion to products. There are a number of approaches for performing such experiments, including the use of sealed glass ampoules (flame sealed under vacuum) that fit perfectly into a MAS rotor (122-124) or tightly sealed NMR rotors prepared using specialist vacuum line apparatus, *e.g.*, the Cryogenic Adsorption Vessel Enabling Rotor Nestling (CAVERN) apparatus.(125-129) In each case, after calcination of the catalyst and adsorption of the reactant molecules, the ampoule or rotor is sealed to maintain the sample integrity and keep the reaction conditions similar to those within a reactor, *i.e.*, excluding any air or moisture from the system. Using the CAVERN approach, catalysts are cooled during the adsorption process and the rotors are sealed using rotor caps with deformable ridges that create air-tight seals when the cap is driven into the rotor. This technique has greatly simplified sample preparation processes, as there is no need for activated samples to be handled in a glove box before transferring to the MAS rotor. Recent modifications have involved the calcination and loading of catalysts under shallow-bed conditions at temperatures of up to 1000 K.(130,131)

One of the greatest challenges in monitoring adsorption processes is the ability to probe the earliest stages of adsorption. A new experimental strategy was recently proposed in which the species to be adsorbed is sealed in a glass capillary and inserted into a MAS rotor, together with the host material on which the adsorption is to take place. In this capillary vibration method, the adsorption process is triggered by the centripetal force exerted on the sample during MAS, which breaks the capillary and brings the host material and adsorbate in direct contact within the rotor.(108,132) This is particularly popular since it does not require any modifications to conventional NMR instrumentation.

Since the first *in situ* continuous-flow NMR experiments in 1987,(133,134) considerable progress has been made. The development of probes with gas injection lines

fed directly into the base of the MAS rotor enabling reactants to flow over the catalyst and be exhausted from the top of the rotor has revolutionised the field.(107,135,136) These probes were later coupled with analytical techniques such as gas chromatography, UV-Vis spectroscopy and mass spectrometry for online analysis of the exhaust gases and volatile reaction products.(135-138) It is worthwhile noting that whilst flow MAS NMR systems do not exactly reproduce the conditions in real flow catalytic reactors, they do represent a significant step forward, particularly for processes difficult to carry out under batch conditions.

In situ NMR studies have also played a crucial role in our understanding of energy devices, including how they operate and why they fail. *In situ* NMR of lithium-ion batteries and electrochemical capacitors are performed on complete cells placed inside the NMR coil (including coin cells, flat sealed plastic bags or cylindrical cells), connected to a potentiostat and electrochemically cycled. NMR spectra are then acquired as a function of state of charge. The cell design is key and, unlike many other *in situ* approaches, static measurements are used due to practical limitations.(111,139)

In situ NMR approaches have developed to the stage that they are now able to provide unique insight into crystallisation, reactivity and functional performance. With continued development of new pulse sequences and improved hardware, it is anticipated that this currently relatively specialist area will become increasingly popular, enabling the full atomic-level insight of NMR spectroscopy to be exploited.

7. Conclusions and Outlook

Solid-state NMR spectroscopy plays an important role in modern analytical chemistry owing to its capability to provide detailed structural and mechanistic information that is challenging, or impossible, to obtain by other experimental methods. Thanks to ongoing developments in methodology, hardware and complementary techniques, many approaches that have been previously viewed as too complex or specialist are becoming more routine. A particularly prominent example of this is the combination of experiment with theoretical calculations. As described in Section 5, over the last decade such

calculations have transformed the way solid-state NMR experiments are used and how data is interpreted. In many cases, the combination of DFT calculations with NMR experiments now goes far beyond basic spectral assignment, enabling detailed models for disorder, dynamics and mechanistic processes to be obtained.

In terms of future developments in solid-state NMR, as discussed in Sections 3 and 6, the areas currently attracting the most widespread attention are the significant sensitivity gains that are obtained using DNP and the application of *in situ* techniques. These both involve significant challenges from the point of view of sample preparation and hardware development (and considerable cost commitments) and it is perhaps at present unclear if they will ever become truly "routine". However, given the current intense interest and rapid pace of development in these areas, we certainly envisage that they will become much more widely accessible in the coming years, and their potential will start to be more fully exploited.

Although NMR spectroscopy offers significant advantages for the study of solid-state structure, it has yet to reach the widespread use or recognition achieved by its solution-state relation. However, we believe we are at a turning point in the history of solid-state NMR - on the brink of the tantalising prospect that this technique will take its deserved place alongside the established "go to" methods for characterising solids. Solid-state NMR will provide not just an alternative, complementary approach, but a comprehensive technique, offering truly novel information. Development will undoubtedly continue, driven by evermore demanding applications, and the growing need for more detailed information on chemical structure and reactivity. We look forward to seeing the exciting role solid-state NMR has to play in solving diverse, and increasingly complex, problems across the chemical, geological, biological and materials sciences.

References

1. Bloch F, Hansen WW, Packard M. 1946. Nuclear induction. *Phys. Rev.* 69:127

2. Purcell E, Torry HC, Pound RV. 1946. Resonance absorption by nuclear magnetic moments in a solid. *Phys. Rev.* 69:37

3. Apperley DC, Harris RK, Hodgkinson P. 2012. *Solid State NMR Basic Principles and Practice*. New York: Momentum Press

4. MacKenzie KJD, Smith ME. 2002. *Multinuclear Solid-State NMR of Inorganic Materials*. Oxford: Pergamon Press

5. Ashbrook SE, Dawson DM, Griffin JM. 2013. Solid-state nuclear magnetic resonance spectroscopy. In *Local Structural Characterisation*, ed. DW Bruce, D O'Hare, RI Walton, pp 1-88. Chichester: Wiley

6. Harris RK, Wasylishen RE, Duer MJ. eds. 2009. *NMR Crystallography*. Hoboken: John Wiley & Sons

7. Martineau C, Senker J, Taulelle F. 2014. NMR crystallography. *Annu. Rep. NMR Spectrosc.* 2014, 82:1-57.

8. Bonhomme C, Gervais C, Babonneau F, Coelho C, Pourpoint F, Azais T, Ashbrook SE, Griffin JM, Yates JR, Mauri F, Pickard CJ. 2012. First-principles calculation of NMR parameters using the gauge including projector augmented wave method: A chemist's point of view. *Chem. Rev.* 112:5733-79

9. Ashbrook SE, McKay D. 2016. Combining solid-state NMR spectroscopy with first-principles calculations – a guide to NMR crystallography. *Chem. Commun.* 52:7186-204

10. Pickard CJ, Mauri F. 2001. All-electron magnetic response with pseudopotentials: NMR chemical shifts. *Phys. Rev. B* 63:245101

11. Yates JR, Pickard CJ, Mauri F. 2007. Calculation of NMR chemical shifts for extended systems using ultrasoft pseudopotentials. *Phys. Rev. B* 76:024401

12. Andrew ER, Bradbury A, Eades RG. 1958. Nuclear magnetic resonance spectra from a crystal rotated at high speed. *Nature*. 182:1659

13. Wasylishen RE, Ashbrook SE, Wimperis S. eds. 2012. *NMR of Quadrupolar Nuclei in Solid Materials*. Chichester: John Wiley & Sons

14. Ashbrook SE, Sneddon S. 2014. New methods and applications in solid-state NMR spectroscopy of quadrupolar nuclei. *J. Am. Chem. Soc.* 136:15440-456

15. Samoson A, Lippmaa E, Pines A. 1988. High resolution solid-state NMR Averaging of second-order effects by means of a double-rotor. *Mol. Phys.* 65:1013-18

16. Llor A, Virlet J. 1988. Towards high-resolution NMR of more nuclei in solids: Sample spinning with time-dependent spinner axis angle. *Chem. Phys. Lett.* 152:248-53

17. Frydman L, Harwood JS. 1995. Isotropic spectra of half-integer quadrupolar spins from bidimensional magic-angle spinning NMR. *J. Am. Chem. Soc.* 117:5367-68

18. Goldburt A, Madhu PK. 2005. Multiple-quantum magic-angle spinning: high-resolution solid-state NMR of half-integer spin quadrupolar nuclei. *Ann. Rep. NMR Spectrosc*. 54:81-153

19. Ashbrook SE, Cutajar M, Pickard CJ, Walton RI, Wimperis S. 2008. Structure and NMR assignment in calcined and as-synthesized forms of AlPO-14: a combined study by first-principles calculations and high-resolution ^{27}Al–^{31}P MAS NMR correlation. *Phys. Chem. Chem. Phys.* 10:5754-64

20. Gan Z. 2000. Isotropic NMR Spectra of half-integer quadrupolar nuclei using satellite transitions and magic-angle spinning. *J. Am. Chem. Soc.* 122:3242-43

21. Ashbrook SE, Wimperis S. 2004. High-resolution NMR of quadrupolar nuclei in solids: the satellite-transition magic angle spinning (STMAS) experiment. *Prog. Nucl. Magn. Reson. Spectrosc.* 45:53-108

22. Hodgkinson P. 2005. Heteronuclear decoupling in the NMR of solids. *Prog. Nucl. Magn. Reson. Spectrosc.* 46:197-222

23. Madhu PK. 2009. High-resolution solid-state NMR spectroscopy of protons with homonuclear dipolar decoupling schemes under magic-angle spinning. *Solid State Nucl. Magn. Reson.* 35:2-11

24. Sakellariou D, Lesage A, Hodgkinson P, Emsley L. 2000. Homonuclear dipolar decoupling in solid-state NMR using continuous phase modulation. *Chem. Phys. Lett.* 319:253-60

25. Pines A, Gibby MG, Waugh JS. 1972. Proton-enhanced nuclear induction spectroscopy. A method for high resolution NMR of dilute spins in solids. *J. Chem. Phys.* 56:1776-77

26. Lesage A. 2009. Recent advances in solid-state NMR spectroscopy of spin I=1/2 nuclei. *Phys. Chem. Chem. Phys.* 32:6876-91

27. Amoureux JP, Trebosc J, Delevoye L, Lafon O, Hu B, Wang Q. 2009. Correlation NMR spectroscopy involving quadrupolar nuclei. *Solid State Nucl. Magn. Reson.* 35:12-18

28. Cavadini S. 2010. Indirect detection of nitrogen-14 in solid-state NMR spectroscopy. *Prog. Nucl. Magn. Reson. Spectrosc.* 56:46-77

29. Pandey MK, Kato H, Ishii Y, Nishiyama Y. 2016. Two-dimensional proton-detected Cl-35/H-1 correlation solid-state NMR experiment under fast magic angle sample spinning: application to pharmaceutical compounds. *Phys. Chem. Chem. Phys.* 8:6209-16

30. Veinberg SL, Johnston KE, Jaroszewicz MJ, Kispal BM, Mireault CR, Kobayashi T, Pruski M, Schurko RW. 2016. Natural abundance ^{14}N and ^{15}N solid-state NMR of pharmaceuticals and their polymorphs. *Phys. Chem. Chem. Phys.* 18:17713-30

31. Levitt MH. 2007. Symmetry-based pulse sequences in magic-angle spinning solid-state NMR. In *Encyclopedia of Magnetic Resonance*. ed. RK Harris and RE Wasylishen, Chichester: John Wiley DOI: 10.1002/9780470034590.emrstm0551

32. Schurko RW. 2013. Ultra-wideline solid-state NMR spectroscopy. *Acc. Chem. Res.* 46:1985-95

33. O'Dell LA, Schurko RW. 2008. QCPMG using adiabatic pulses for faster acquisition of ultra-wideline NMR spectra. *Chem. Phys. Lett.* 464:97-102

34. Johnston KE, O'Keefe CA, Gauvin RM, Trebosc J, Delevoye L, Amoureux JP, Popoff N, Taouvik M, Oudatchin K, Schurko RW. 2013. A study of transition-metal organometallic complexes combining ^{35}Cl solid-state NMR spectroscopy and first-principles DFT calculations. *Chem. Eur. J.* 19:12396-414

35. Harris KJ, Lupulescu A, Lucier BEG, Frydman L, Schurko RW. 2012. Broadband adiabatic inversion pulses for cross polarization in wideline solid-state NMR spectroscopy. *J. Magn. Reson.* 224:38-47

36. Nakashima TT, Wasylishen RE. 2011. Sensitivity and resolution enhancement of half-integer quadrupolar nuclei in solid-state NMR. In *Encyclopedia of Magnetic Resonance*. ed. RK Harris and RE Wasylishen, Chichester: John Wiley DOI: 10.1002/9780470034590.emrstm1200

37. Burum DP. 2007. Cross polarisation in solids. In *Encyclopedia of Magnetic Resonance*, ed. RK Harris, RE Wasylishen. Chichester: John Wiley

38. Ashbrook SE, Wimperis S. 2000. Single- and multiple-quantum cross-polarization in NMR of quadrupolar nuclei in static samples. *Mol. Phys.* 98:1-26

39. Amoureux JP, Pruski M. 2002. Theoretical and experimental assessment of single- and multiple-quantum cross-polarization in solid state NMR. *Solid State Nucl. Magn. Reson.* 7:327-31

40. Ashbrook SE, Wimperis S. 2004. Spin-locking of half-integer quadrupolar nuclei in nuclear magnetic resonance of solids: Creation and evolution of coherences. *J. Chem. Phys.* 120:2719-31

41. Meiboom S, Gill D. 1958. Modified spin-echo method for measuring nuclear relaxation times. *Rev. Sci. Instrum.* 29:688-91

42. Carr HY, Purcell EM. 1954. Effects of diffusion on free precession in nuclear magnetic resonance experiments. *Phys. Rev.* 94:630-38

43. Siegel R, Nakashima TT, Wasylishen RE. 2004. Application of multiple-pulse experiments to characterize broad NMR chemical-shift powder patterns from spin-1/2 nuclei in the solid state. *J. Phys. Chem. B* 108:2218-26

44. Hung I, Rossini AJ, Schurko RW. 2004. Application of the Carr−Purcell Meiboom−Gill pulse sequence for the acquisition of solid-state NMR spectra of spin-1/2 nuclei. *J. Phys. Chem. A* 108:7112-20

45. Ashbrook SE, Mitchell MR, Sneddon S, Moran RF, de los Reyes M, Lumpkin GR, Whittle KR. 2015. New insights into phase distribution, phase composition and disorder in $Y_2(Zr,Sn)_2O_7$ ceramics from NMR spectroscopy. *Phys. Chem. Chem. Phys.* 17:9049-59

46. Larsen FH, Jakobsen HJ, Ellis PD, Nielsen NC. 1997. Sensitivity-enhanced quadrupolar-echo NMR of half-integer quadrupolar nuclei. Magnitudes and relative orientation of chemical shielding and quadrupolar coupling tensors. *J. Phys. Chem. A* 101:8597-606

47. Hung I, Gan Z. 2010. On the practical aspects of recording wideline QCPMG NMR spectra. *J. Magn. Reson.* 204:256-65

48. Griffin JM, Berry AJ, Ashbrook SE. 2011. Observation of "hidden" magnesium: First-principles calculations and ^{25}Mg solid-state NMR of enstatite. *Solid State Nucl. Magn. Reson.* 40:91-9

49. Vosegaard T, Larsen FH, Jakobsen HJ, Ellis PD, Nielsen NC. 1997. Sensitivity-enhanced multiple-quantum MAS NMR of half-integer quadrupolar nuclei. *J. Am. Chem. Soc.* 119:9055-56

50. Kentgens APM, Verhagen R. 1999. Advantages of double frequency sweeps in static, MAS and MQMAS NMR of spin I = 3/2 nuclei. *Chem. Phys. Lett.* 300:435-43

51. Madhu PK, Goldbourt A, Frydman L, Vega S. 1999. Sensitivity enhancement of the MQMAS NMR experiment by fast amplitude modulation of the pulses. *Chem. Phys. Lett.* 307:41-7

52. Madhu PK, Goldbourt A, Frydman L, Vega S. 2000. Fast radio-frequency amplitude modulation in multiple-quantum magic-angle-spinning nuclear magnetic resonance: Theory and experiments. *J. Chem. Phys.* 112:2377-91

53. Colaux H, Dawson DM, Ashbrook SE. 2014. Efficient amplitude-modulated pulses for triple- to single-quantum coherence conversion in MQMAS NMR. *J. Phys. Chem. A* 118:6018-25

54. Colaux H, Dawson DM, Ashbrook SE. 2017. Investigating FAM-N pulses for signal enhancement in MQMAS NMR of quadrupolar nuclei. *Solid State Nucl. Magn. Reson.* In press (http://dx.doi.org/10.1016/j.ssnmr.2017.01.001)

55. Ni QZ, Daviso E, Can TV, Markhasin E, Jawla SK, Swager, TM, Temkin RJ, Herzfeld J, Griffin RG. 2013. High frequency dynamic nuclear polarization. *Acc. Chem. Res.* 46:1933-41

56. Rossini AJ, Zagdoun A, Lelli M, Lesage A, Copéret C, Emsley L. 2013. Dynamic nuclear polarization surface enhanced NMR spectroscopy. *Acc. Chem. Res.* 46:1942-51

57. Marker K, Paul S, Fernandez-de-Alba C, Lee D, Mouesca J-M, Hediger S, De Paëpe G. 2017. Welcoming natural isotopic abundance in solid-state NMR: probing π-stacking and supramolecular structure of organic nanoassemblies using DNP. *Chem. Sci.* 8:974-87

58. Song C, Hu K-N, Joo C-G, Swager TM, Griffin RG. 2006. TOTAPOL: A biradical polarizing agent for dynamic nuclear polarization experiments in aqueous media. *J. Am. Chem. Soc.* 128:11385-90

59. Hu K-N, Yu H-H, Swager TM, Griffin RG. 2004. Dynamic nuclear polarization with biradicals. *J. Am. Chem. Soc.* 126:10844-45

60. Blanc F, Sperrin L, Jefferson DA, Pawsey S, Rosay M, Grey CP. 2013. Dynamic nuclear polarization enhanced natural abundance O-17 spectroscopy. *J. Am. Chem. Soc.* 135:2975-78

61. Perras FA, Chaudhary U, Slowing II, Pruski M. 2016. Probing surface hydrogen bonding and dynamics by natural abundance, multidimensional, O-17 DNP-NMR spectroscopy. *J. Phys. Chem. C* 120:11535-44

62. Rossini AJ, Schlagnitweit J, Lesage A, Emsley L. 2015. High-resolution NMR of hydrogen in organic solids by DNP enhanced natural abundance deuterium spectroscopy. *J. Magn. Reson.* 259:192-98

63. Moran RF, Dawson DM, Ashbrook SE. 2017. Exploiting NMR spectroscopy for the study of disorder in solids. *Int. Rev. Pys. Chem*. 36:39-115.

64. Griffin JM, Yates JR, Berry AJ, Wimperis S, Ashbrook SE. 2010. High-resolution ^{19}F MAS NMR spectroscopy: Structural disorder and unusual J couplings in a fluorinated hydroxy-silicate. *J. Am. Chem. Soc.* 132:15651-60

65. Ashbrook SE, Whittle KR, Lumpkin GR, Farnan I. 2006. ^{89}Y magic-angle spinning NMR of $Y_2Ti_{2-x}Sn_xO_7$ pyrochlores. *J. Phys. Chem. B* 110:10358-64

66. Reader SW, Mitchell MR, Johnston KE, Pickard CJ, Whittle KR, Ashbrook SE. 2009. Cation disorder in pyrochlore ceramics: ^{89}Y MAS NMR and first-principles calculations. *J. Phys. Chem. C* 113:18874-83

67. Massiot D, Fayon F, Capron M, King I, Le Calve S, Alonso B, Durand JO, Bujoli B. Gan ZH, Hoatson, G. 2002. Modelling one-and two-dimensional solid-state NMR spectra. *Magn. Reson. Chem.* 40:70-6

68. Czjzek G, Fink J, Götz F, Schmidt H, Coey JMD. 1981. Atomic coordination and the distribution of electric field gradients in amorphous solids. *Phys. Rev. B* 23:2513-30

69. Le Caer G, Bureau B, Massiot D. 2010. An extension of the Czjzek model for the distributions of electric field gradients in disordered solids and an application to NMR spectra of ^{71}Ga in chalcogenide glasses. *J. Phys.: Condens. Matter* 22:065401

70. Duer MJ. 2004. *Introduction to solid-state NMR spectroscopy*. Blackwell, Oxford

71. Batchelder LS. 2007. Deuterium NMR in solids. In *eMagRes*: John Wiley & Sons, Ltd

72. Mowat JPS, Miller SR, Griffin JM, Seymour VR, Ashbrook SE, Thompson SP, Fairen-Jimenez D, Banu A-M, Duren T, Wright PA. 2011. Structural chemistry, monoclinic-to-orthorhombic phase transition, and CO_2 adsorption behavior of the small pore scandium terephthalate, $Sc_2(O_2CC_6H_4CO_2)_3$, and its nitro- and amino-functionalized derivatives. *Inorg. Chem.* 50:10844-58

73. Griffin JM, Miller AJ, Berry AJ, Wimperis S, Ashbrook SE. 2010. Dynamics on the microsecond timescale in hydrous silicates studied by solid-state ^2H NMR spectroscopy. *Phys. Chem. Chem. Phys.* 12:2989-98

74. Dawson DM, Griffin JM, Seymour VR, Wheatley PS, Amri M, Kurkiewicz K, Guillou N, Wimperis S, Walton RI. 2017. A Multinuclear NMR study of six forms of AlPO-34: structure and motional broadening. *J. Phys. Chem. C* 121:1781-93

75. Martineau C. 2014. NMR crystallography: Applications to inorganic materials. *Solid State Nucl. Magn. Reson*. 63-64:1-12

76. Mafra L. (Editor). 2015. NMR Crystallography, Special Edition *Solid State Nucl. Magn. Reson*. 65:1-132

77. Bryce DL. 2017. NMR crystallography: structure and properties of materials from solid-state nuclear magnetic resonance observables. *IUCrJ*. 4:350-9

78. Pöppler AC, Corlett EK, Pearce H, Seymour MP, Reid M, Montgomery MG, Brown SP. 2017. Single-crystal X-ray diffraction and NMR crystallography of a 1:1 cocrystal of dithianon and pyrimethanil. *Acta Cryst. C* 73:149-156

79. Widdifield CM, Robson H, Hodgkinson P. 2016. Furosemide's one little hydrogen atom: NMR crystallography structure verification of powdered molecular organics. *Chem. Commun*. 52:6685-8

80. Fernandes A, McKay D, Sneddon S, Dawson DM, Lawson S, Veazey R, Whittle KE, Ashbrook SE. 2016. Phase composition and disorder in $La_2(Sn,Ti)_2O_7$ ceramics: new insights from NMR crystallography. *J. Phys. Chem. C* 120:20288-96

81. Brouwer DH, Cadars S, Hotke K, Van Huizen J, Van Huizen N. 2017. Structure determination of a partially ordered layered silicate material with an NMR crystallography approach. *Acta Cryst. C* 73:126-7

82. Bouchevreau B, Martineau C, Mellot-Draznieks C, Tuel A, Suchomel MR, Trébosc J, Lafon O, Amoureux JP, Taulelle F. 2013. High-resolution structural characterization of two layered aluminophosphates by synchrotron powder diffraction and NMR crystallographies. *Chem. Mater*. 25:2227-42

84. Harris RK, Hodgkinson P, Pickard CJ, Yates JR, Zorin V. 2007. Chemical shift computations on a crystallographic basis: some reflections and comments. *Magn. Reson. Chem*. 45:S174-86

85. Byrne PJ, Warren JE, Morris RE, Ashbrook SE. 2009. Structure and NMR assignment in $AlPO_4$-15: A combined study by diffraction, MAS NMR and first-principles calculations. *Solid State Sci*. 11:1001-06

86. Brouwer DH, Langendoen KP, Ferrant Q. 2011. Measurement and calculation of ^{13}C chemical shift tensors in α-glucose and α-glucose monohydrate. *Can. J. Chem*. 89:737-44

87. Sneddon S, Dawson DM, Pickard CJ, Ashbrook SE. 2014. Calculating NMR parameters in aluminophosphates: evaluation of dispersion correction schemes. *Phys. Chem. Chem. Phys*. 16:2660-73

88. Klimeš J, Michaelides A. 2012. Perspective: Advances and challenges in treating van der Waals dispersion forces in density functional theory. *J. Chem. Phys.* 137:120901

89. Grimme S. 2006. Semiempirical GGA-type density functional constructed with a long-range dispersion correction. *J. Comput. Chem*. 27:1787-99

90. Tkatchenko A, Scheffler M. 2009. Accurate molecular van der Waals interactions from ground-state electron density and free-atom reference data. *Phys. Rev. Lett*. 102:073005

91. Dudenko DV, Yates JR, Harris KDM, Brown SP. 2013. An NMR crystallography DFT-D approach to analyse the role of intermolecular hydrogen bonding and π- π interactions in driving cocrystallisation of indomethacin and nicotinamide. *CrystEngComm*. 15:8797-807

92. Folliet N, Gervais C, Costa D, Laurent G, Babonneau F, Stievano L, Lambert JF, Tielens F. 2013. A molecular picture of the adsorption of glycine in mesoporous silica through NMR experiments combined with DFT-D calculations. *J. Phys. Chem. C* 117:4104-14

93. Mowat JPS, Seymour VR, Griffin JM, Thompson SP, Slawin AMZ, Fairen-Jimenez D, Duren T, Ashbrook SE, Wright PA. 2012. A novel structural form of MIL-53 observed for

the scandium analogue and its response to temperature variation and CO_2 adsorption. *Dalton Trans*. 41:3937-41

94. Day GM. 2011. Current approaches to predicting molecular organic crystal structures. *Crystallogr. Rev*. 17:3-52

95. Pickard CJ, Needs RJ. 2011. *Ab initio* random structure searching. *J. Phys.: Condens. Matter* 23:053201

96. Clark SJ, Segall MD, Pickard CJ, Hasnip PJ, Probert MIJ, Refson K, Payne MC. 2005. First principles methods using CASTEP. *Z. Kristallogr*. 220:567-70

97. Mayo M, Morris AJ. 2017. Structure prediction of Li-Sn and Li-Sb Intermetallics for lithium-ion batteries anodes. *Chem. Mater.* 29:5787-95

98. Moran RF, McKay D, Pickard CJ, Berry AJ, Griffin JM, Ashbrook SE. 2016. Hunting for hydrogen: random structure searching and prediction of NMR parameters of hydrous wadsleyite. *Phys. Chem. Chem. Phys.* 18:10173-81

99. Griffin JM, Berry AJ, Frost DJ, Wimperis S, Ashbrook SE. 2013. Water in the Earth's mantle: a solid-state NMR study of hydrous wadsleyite. *Chem. Sci.* 4:1523-1538

100. Ashbrook SE, Dawson DM. 2013. Exploiting periodic first-principles calculations in NMR spectroscopy of disordered solids. *Acc. Chem. Res.* 46:1964-74

101. Seymour VR, Eschenroeder ECV, Castro M, Wright PA, Ashbrook SE. 2013. Application of NMR crystallography to the determination of the mechanism of charge-balancing in organocation-templated AlPO STA-2. *CrystEngComm* 15:8668-79

102. Dervişoğlu R, Middlemiss DS, Blanc F, Lee YL, Morgan D, Grey CP. 2015. Joint experimental and computational ^{17}O and ^{1}H solid state NMR study of $Ba_2In_2O_4(OH)_2$ structure and dynamics. *Chem. Mater.* 27:3861-73

103. Cadars S, Allix M, Brouwer DH, Shayib R, Suchomel M, Garaga MN, Rakhmatullin A, Burton AW, Zones SI, Massiot D, Chmelka BF. 2014. Long- and short-range constraints for the structure determination of layered silicates with stacking disorder. *Chem. Mater.* 26:6994-7008

104. Stebbins JF, McCarty RJ, Palke AC. 2017. Solid-state NMR and short-range order in crystalline oxides and silicates: a new tool in paramagnetic resonances. *Acta Cryst. C* 73:128-36

105. Seymour ID, Middlemiss DS, Halat DM, Trease NM, Pell AJ, Grey CP. 2016. Characterizing oxygen local environments in paramagnetic battery materials via ^{17}O NMR and DFT calculations. *J. Am. Chem. Soc*. 138:9405-08

106. Pienack N, Bensch W. 2011. *In-situ* monitoring of the formation of crystalline solids. *Angew. Chem. Int. Ed.* 50:2014-34.

107. Hunger M, Horvath T. 1995. A new MAS NMR Probe for *in situ* investigations of hydrocarbon conversion on solid catalysts under continuous-flow conditions. *J. Chem. Soc., Chem. Commun*. 1423-24

108. Xu M, Harris KDM, Thomas JM, Vaughan DEW. 2007. Probing the evolution of adsorption on nanoporous solids by *in situ* solid-state NMR spectroscopy. *ChemPhysChem*. 8:1311-13

109. Hunger M, Wang W. 2006. Characterization of solid catalysts in the functioning state by nuclear magnetic resonance spectroscopy. *Adv. Catal.* 50:149-225

110. Zheng A, Huang SJ, Wang Q, Zhang H, Deng F, Liu SB. 2013. Progress in development and application of solid-state NMR for solid acid catalysis. *Chin. J. Catal.* 34:436-91

111. Blanc F, Leskes M, Grey CP. 2013. *In situ* solid-state NMR spectroscopy of electrochemical cells: batteries, supercapacitors and fuel cells. *Acc. Chem. Res.* 46:1952-63

112. Hughes CE, Williams PA, Keast VL, Charalampopoulos VG, Edwards-Gau GR, Harris KDM. 2015. New *in situ* solid-state NMR techniques for probing the evolution of crystallization processes: pre-nucleation, nucleation and growth. *Faraday Discuss.* 179:115-40

113. Hughes CE, Harris KDM. 2008. A technique for *in situ* monitoring of crystallization from solution by solid-state ^{13}C CPMAS NMR spectroscopy. *J. Phys. Chem. A*. 112:6808-10

114. Hughes CE, Harris KDM. 2010. Direct observation of a transient polymorph during crystallization. *Chem. Commun.* 46:4982-84

115. Hughes CE, Williams PA, Harris KDM. 2014. "CLASSIC NMR": An *in-situ* NMR strategy for mapping the time-evolution of crystallization processes by combined liquid-state and solid-state measurements. *Angew. Chem. Int. Ed.* 53:8939-43

116. Harris KDM, Hughes CE, Williams PA. 2015. Monitoring the evolution of crystallization processes by *in-situ* solid-state NMR spectroscopy. *Solid State Nucl. Magn. Reson*. 65:107-13

117. Hunger M. 2008. *In situ* flow MAS NMR spectroscopy: State of the art applications in heterogeneous catalysis. *Prog. Nucl. Magn. Reson. Spectrosc.* 53:105-27

118. Ivanova II, Kolyagin YG. 2010. Impact of *in situ* MAS NMR techniques to the understanding of the mechanisms of zeolite catalysed reaction. *Chem. Soc. Rev.* 39:5018-50

119. Wang W, Hunger M. 2008. Reactivity of surface alkoxy species on acidic zeolite catalysts. *Acc. Chem. Res.* 41:895-904

120. Derouane EG, He H, Derouane-Abd Hamid SB, Lambert D, Ivanova I. 2000. *In situ* MAS NMR spectroscopy study of catalytic reaction mechanisms. *J. Mol. Catal. A: Chem.* 158:5-17

121. Zhang W, Xu S, Han X, Bao X. 2012. *In situ* solid-state NMR for heterogeneous catalysis: a joint experimental and theoretical approach. *Chem. Soc. Rev.* 41:192-210

122. Gay ID. 1984. A magic-angle spinner for vacuum-sealed samples. *J. Magn. Reson*. 58:413-20

123. Anderson MW, Klinowski J. 1989. Direct observation of shape selectivity in zeolite ZSM-5 by magic-angle-spinning NMR. *Nature.* 339:200-3

124. Carpenter TA, Klinowski J, Tilak D, Tennakoon B, Smith CJ, Edwards DC. 1986. Sealed capsules for convenient acquisition of variable-temperature controlled-atmosphere magic-angle-spinning NMR spectra of solids. *J. Magn. Reson.* 68:561-3

125. Haw JF, Richardson BR, Oshiro IS, Lazo ND, Speed JA. 1989. Reactions of propene on Zeolite HY catalyst studied by *in situ* variable-temperature solid-state nuclear magnetic resonance spectroscopy. *J. Am. Chem. Soc.* 111:2052-58

126. Richardson BR, Lazo ND, Schettler PD, White JL, Haw JF. 1990. Reactions of butadiene in zeolite catalysts by *in situ* variable-temperature solid-state nuclear magnetic resonance spectrometry. *J. Am. Chem. Soc.* 112:2886-91

127. Munson EJ, Ferguson DB, Kheir AA, Haw JF. 1992. Applications of a new CAVERN design to the study of reactions on catalysts using *in situ* solid-state NMR. *J. Catal*. 136:504-9

128. Xu T, Haw JF. 1997. The development and applications of CAVERN methods for *in situ* NMR studies of reactions on solid acids. *Top. Catal.* 4:109-18

129. Munson EJ, Murray DK, Haw JF. 1993. Shallow-bed CAVERN design for *in situ* solid-state NMR studies of catalytic reactions. *J. Catal.* 141:733-6

130. Zhang WP, Ma D, Liu XC, Liu XM, Bao XH. 1999. Perfluorotributylamine as a probe molecule for distinguishing internal and external acidic sites in zeolites by high-resolution ^{1}H MAS NMR spectroscopy. *Chem. Commun.* 1091-2

131. Ma D, Shu YY, Zhang WP, Han XW, Xu YD, Bao XH. 2000. *In situ* ^{1}H MAS NMR spectroscopic observation of proton species on a Mo-modified HZSM-5 zeolite catalyst for the dehydroaromatization of methane. *Angew. Chem., Int. Ed.* 39:2928-31

132. Xu M, Harris KDM, Thomas JM. 2008. Mapping the evolution of adsorption of water in nanoporous silica by *in situ* solid-state ^{1}H NMR spectroscopy. *J. Am. Chem. Soc.* 130:5880-2

133. Haddix GW, Reimer JA, Bell AT. 1987. A nuclear magnetic resonance probe for *in situ* studies of adsorbed species on catalysts. *J. Catal.* 106:111-5

134. Haddix GW, Reimer JA, Bell AT. 1987. Characterization of H_2 adsorbed on γ-Mo_2N by NMR spectroscopy. *J. Catal.* 108:50-4

135. Hunger M, Seiler M, Horvath T. 1999. A technique for simultaneous *in situ* MAS NMR and on-line gas chromatographic studies of hydrocarbon conversions on solid catalysts under flow conditions. *Catal. Lett.* 57:199-204

136. Goguen P, Haw JF. 1996. An *in situ* NMR probe with reagent flow and magic angle spinning. *J. Catal*. 161:870-2.

137. Hunger M, Horvath T. 1997. Conversion of propan-2-ol on zeolites LaNaY and HY investigated by gas chromatography and *in situ* MAS NMR spectroscopy under continuous-flow conditions. *J. Catal*. 167:187-97

138. Hunger M, Wang W. 2004. Formation of cyclic compounds and carbenium ions by conversion of methanol on weakly dealuminated zeolite H-ZSM-5 investigated via novel *in situ* CF MAS NMR/UV-Vis technique. *Chem. Commun.* 584-5

139. Griffin JM, Forse AC, Grey CP. 2016. Solid-state NMR studies of supercapacitors. *Solid State Nucl. Magn. Reson.* 74:16-35

Figure Captions

Figure 1. ^{1}H (I = 1/2, 14.1 T) solid-state NMR spectra of theobromine. In (a), the sample is static, while in (b) 12.5 kHz MAS, (c) 40 kHz MAS and (d) 9.183 kHz MAS with homonuclear ^{1}H decoupling is used. * denote spinning sidebands and † decoupling artifacts.

Figure 2. (a) ^{27}Al (I = 5/2, 14.1 T) MAS and MQMAS NMR spectra of calcined AlPO-14, showing the four crystallographically-distinct Al sites.(19) (b) $^{1}H/^{15}N$ (I = 1/2, 14.1 T) HETCOR NMR spectrum of a pharmaceutical compound. Reproduced from Ref. 30 with permission from the PCCP Owner Societies. (c) ^{35}Cl (I = 3/2, 21.1 T) frequency-stepped WURST CPMG wideline NMR spectrum of a palladium-based catalyst. Reproduced from Ref. 34.

Figure 3. (a) Pulse sequence for a CPMG experiment, where multiple echoes are acquired in one transient. (b) ^{89}Y (I = 1/2, 14.1 T) CPMG MAS NMR spectra of $Y_2Zr_{2-x}Sn_xO_7$ (x = 0.8 and 0.4).(45) (c) ^{25}Mg (I = 5/2, 14.1 T) wideline CPMG NMR spectrum of $MgSiO_3$ enstatite. Reprinted from Ref. 48, with permission from Elsevier. (d) ^{1}H-^{13}C CP MAS spectra of cyclic diphenylalanine nanotubes recorded with (*i.e.*, DNP) and without microwave irradiation. Reproduced from Ref. 57. Published by The Royal Society of Chemistry.

Figure 4. (a) ^{19}F (I = 1/2, 14.1 T) MAS NMR spectrum of $4Mg_2SiO_4.Mg(OH_{0.5}F_{0.5})_2$ showing four different local environments for fluorine species which are distinguished on the basis of the arrangements of adjacent F^-/OH^- species. Adapted with permission from Ref 64. Copyright 2017 American Chemical Society. (b) ^{89}Y (I = 1/2, 14.1 T) MAS NMR spectrum of Y_2SnTiO_7 pyrochlore showing resonances corresponding to different Sn/Ti next nearest neighbour environments. (c) Variable-temperature ^{2}H (I = 1, 9.4 T) NMR spectra of a scandium terephthalate metal-organic framework showing changes in the lineshape due to rotation of the linker. Adapted with permission from Ref. 72. Copyright 2011 American Chemical Society. (d) Variable-temperature ^{27}Al (I = 5/2, 14.1 T) MAS NMR spectra of

AlPO-34 containing dimethylimidazolium and morpholinium. Adapted with permission from Ref. 74. Copyright 2017 American Chemical Society.

Figure 5. Structure searching approach to study the hydration of wadsleyite.(98) (a) Unit cell of β-Mg_2SiO_4 with (b) the AIRSS protocol used to produce 819 structures. (c) Enthalpy ranking of 103 selected structures. (d) Plot of H–O bond length against calculated ^{1}H chemical shifts for low-enthalpy structures. Reproduced (in part) from Ref. 98 with permission of the PCCP Owner Societies.

Figure 6. (a) *In situ* ^{1}H-^{13}C CP NMR spectra, of the crystallisation of α, β and γ polymorphs of glycine from H_2O, D_2O and H_2O/CH_3OH. Adapted from Ref. 112 with permission from The Royal Society of Chemistry. (b) Schematic showing the *in situ* CLASSIC approach,(115) where interleaved solution-state and solid-state (*via* CP) measurements allow the different phases present to be studied simultaneously.

Figure 1

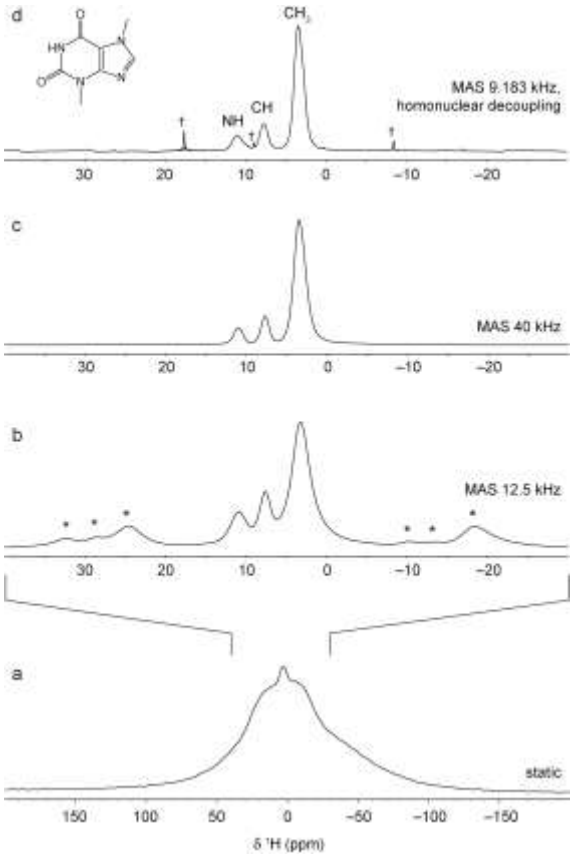
d
CH3
NH
CH
MAS 9.183 kHz,
homonuclear decoupling
30
20
10
0
−10
−20
c
MAS 40 kHz
30
20
10
0
−10
−20
b
MAS 12.5 kHz
30
20
10
0
−10
−20
a
static
150
100
50
0
−50
−100
−150
δ 1H (ppm)

Figure 2

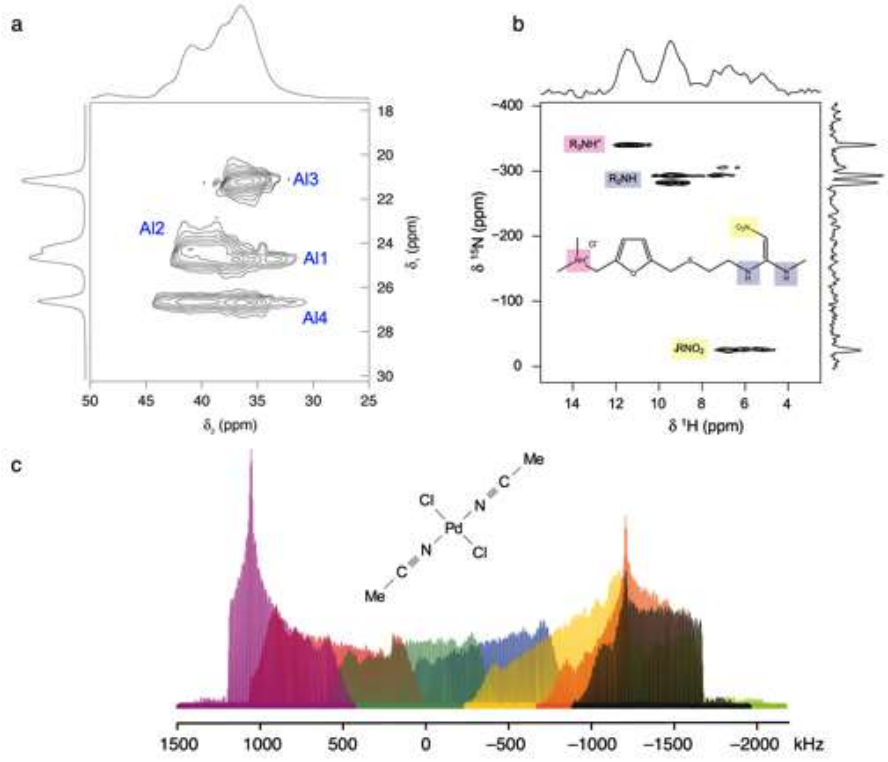
a
Al3
Al2
Al1
Al4
δ2 (ppm)
δ1 (ppm)
b
δ 15N (ppm)
δ 1H (ppm)
c
Cl
Pd
N
C
Me
1500
1000
500
0
−500
−1000
−1500
−2000
kHz

Figure 3

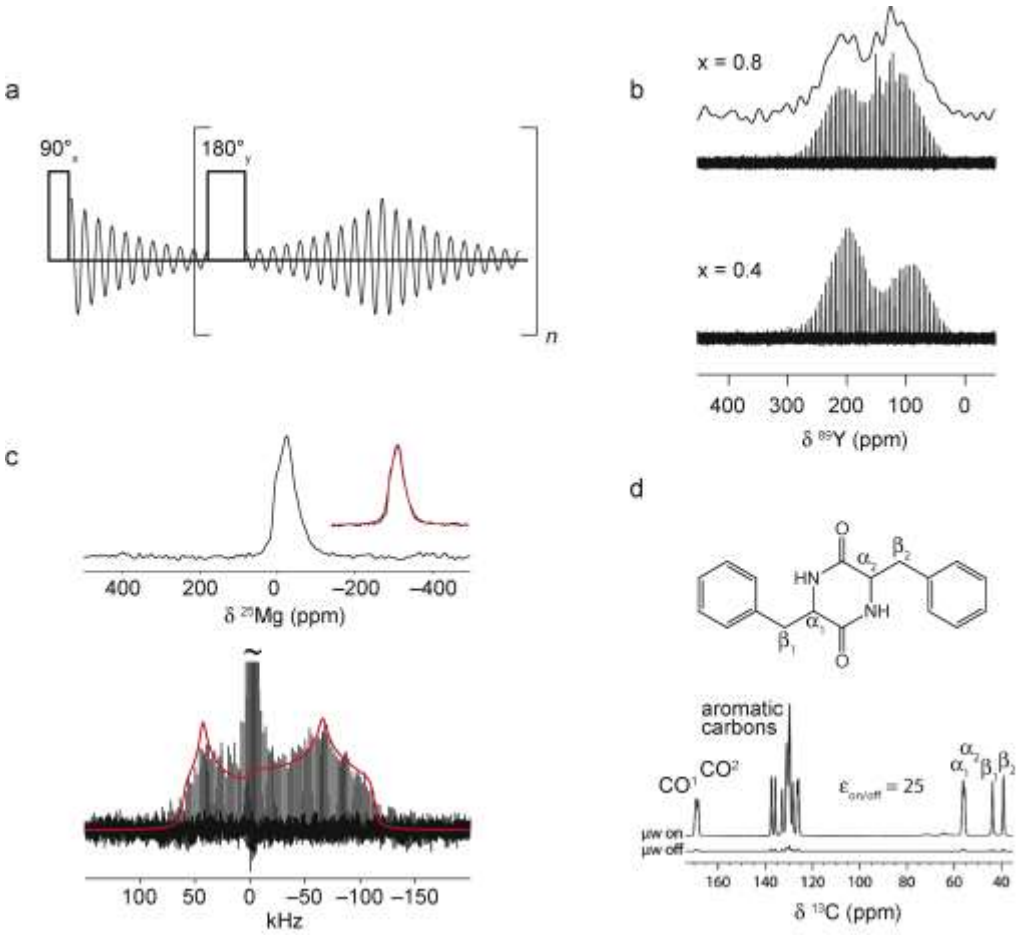
a
90°x
180°y
n
b
x = 0.8
x = 0.4
400 300 200 100 0
δ 89Y (ppm)
c
400 200 0 −200 −400
δ 25Mg (ppm)
100 50 0 −50 −100 −150
kHz
d
HN
NH
O
O
aromatic carbons
CO1
CO2
εon/off = 25
μw on
μw off
160 140 120 100 80 60 40
δ 13C (ppm)

Figure 4

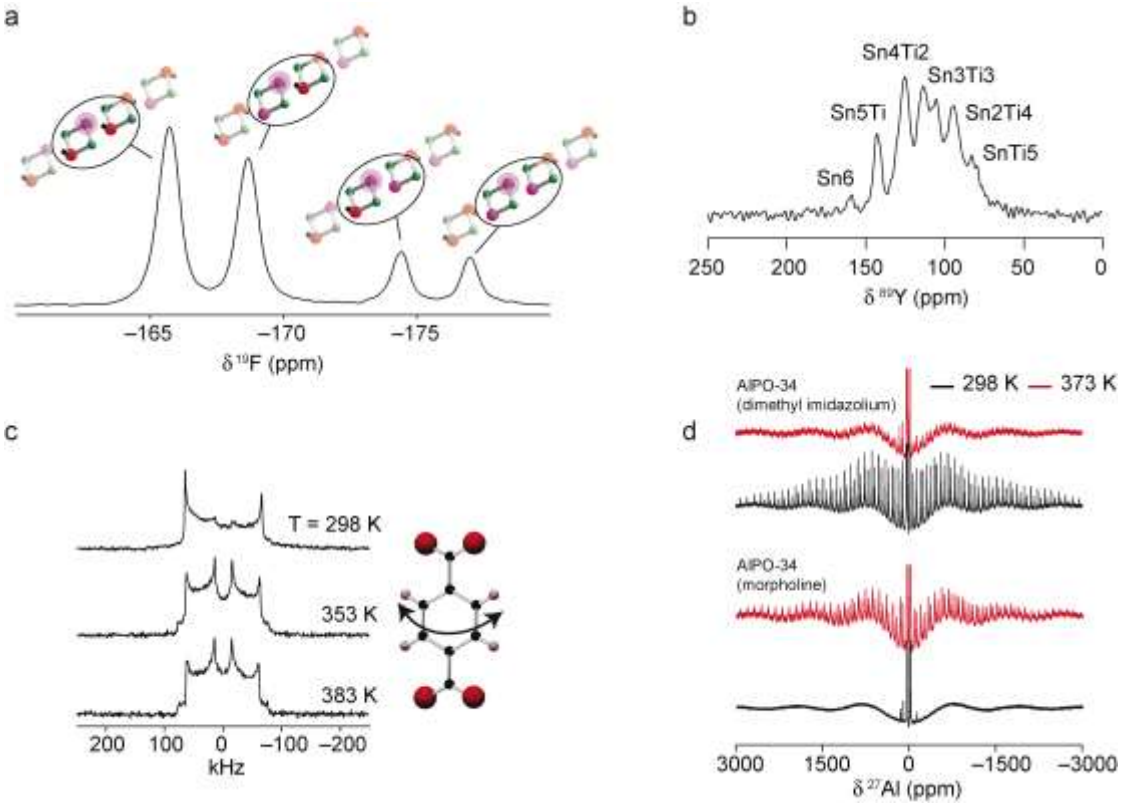
a
−165
−170
−175
δ 19F (ppm)
b
Sn4Ti2
Sn3Ti3
Sn5Ti
Sn2Ti4
SnTi5
Sn6
250
200
150
100
50
0
δ 89Y (ppm)
c
T = 298 K
353 K
383 K
200
100
0
−100
−200
kHz
d
AlPO-34
(dimethyl imidazolium)
298 K
373 K
AlPO-34
(morpholine)
3000
1500
0
−1500
−3000
δ 27Al (ppm)

Figure 5

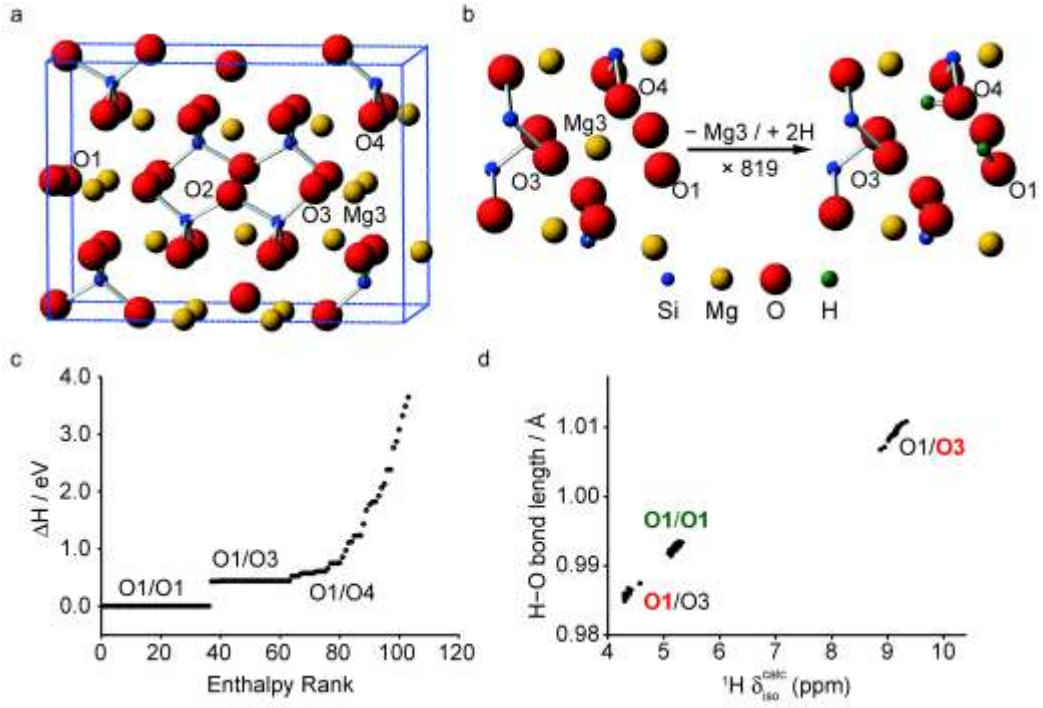
a
O1
O2
O3
Mg3
O4
b
Mg3
O4
O3
O1
− Mg3 / + 2H
× 819
O3
O4
O1
Si
Mg
O
H
c
ΔH / eV
4.0
3.0
2.0
1.0
0.0
O1/O1
O1/O3
O1/O4
0
20
40
60
80
100
120
Enthalpy Rank
d
H–O bond length / Å
1.01
1.00
0.99
0.98
O1/O3
O1/O1
O1/O3
4
5
6
7
8
9
10
¹H δ (ppm)

Figure 6

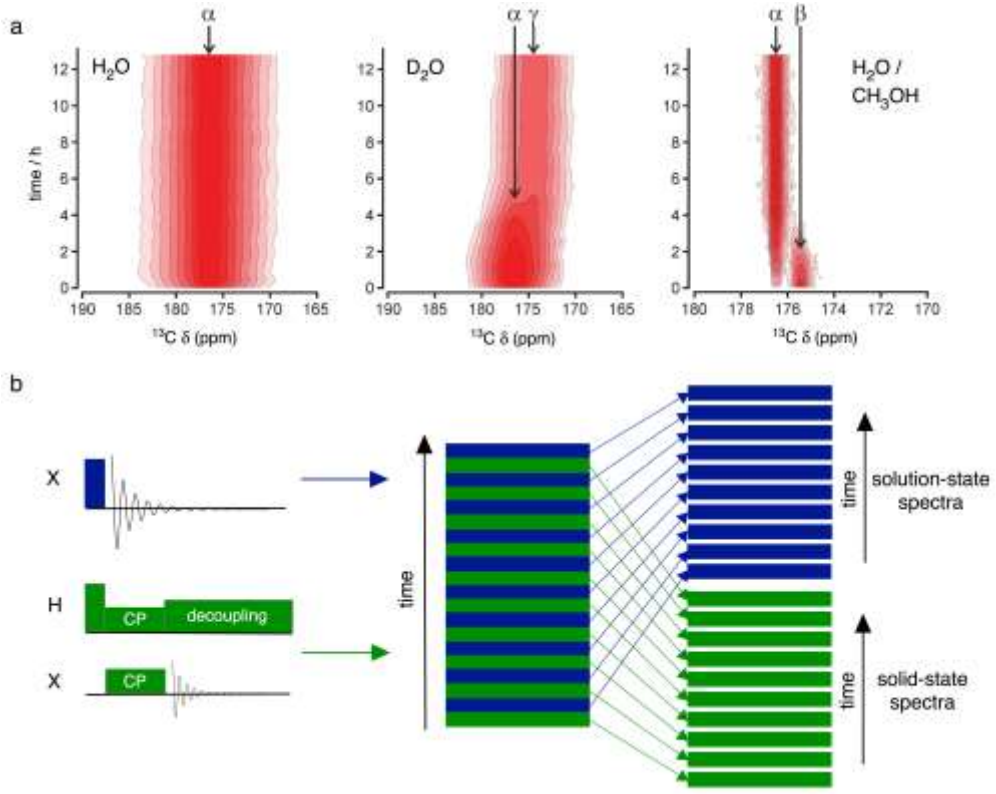
a
α
H2O
time / h
13C δ (ppm)
α γ
D2O
α β
H2O /
CH3OH
b
X
H
CP
decoupling
X
CP
time
solution-state
spectra
solid-state
spectra